compare their antigenicities. We confirmed the antigenicity of the recombinant truncated N proteins by Western blotting using a serum from a convalescent SARS patient. When ELISA reactions using N1 or N3, which had been determined to have antigenicity in the Western blot, were performed with sera from 10 convalescent SARS-CoV patients, the results were all positive. Furthermore, none of the healthy sera reacted positively with N1 or N3 in the ELISA. On the other hand, N2 did not react positively with serum from convalescent SARS-CoV patients in the Western blot.

These data show that the middle or C-terminal regions of SARS-CoV N protein have strong antigenicity, but the N-terminal region of the SARS-CoV N protein has weak antigenicity, as has been reported previously [3, 9, 15]. The sensitivity and specificity of N1 and N3 were each high in ELISA.

A highly conserved motif is present in the N-terminal half of all coronavirus N proteins [6]. Human coronaviruses (HCoVs) are responsible for 10–35% of the upper respiratory tract infections known to cause the common cold, but these infections are not severe [12, 13]. We can distinguish SARS-CoV patients from patients with HCoV infections by the severity of the symptoms. However, a false-positive result is possible in ELISA systems using recombinant N proteins because of cross-reactivity with HCoVs [6, 17, 18]. Yu *et al.* [18] reported that ELISA using NΔ121 protein (122–422 aa) showed a reduced nonspecific reaction compared with ELISA using N protein (5–422 aa), because the N proteins of coronaviruses have a highly conserved motif in the N-terminal half. However, other authors have reported that the possibility of a false-positive result was low, although a full sequenced N protein was used for SARS diagnosis [1, 4, 15]. In this study, although N1 and N3 contain the conserved motif, the ELISA using them did not show false-positive results. However, sera with high titers against HCoVs can react with recombinant N proteins [17].

Therefore, we tried to confirm the specificity of the ELISA that we developed. HCoV-229E- or OC43-infected cell lysate was analyzed by Western blotting using sera from convalescent SARS patients. None of them reacted with HCoV-229E or OC43 (data not shown). In fact, we should have investigated the reactivity of the ELISA with HCoV-infected sera. However, unfortunately, we could not obtain those sera. Instead, we checked the cross-reactivity between HCoV-229E or OC43 and sera from convalescent SARS patients. Abs in convalescent SARS patients did not react with HCoV-229E or OC43. The epitope of N1 or N3 and HCoV-229E or OC43 may be different, because the results of the reactivity with the same Abs (sera from convalescent SARS patients) were different. Therefore, we guess that ELISA using N1 or N3 will not react with sera of HCoV-229E- or OC43-infected patients. However, the cross-reactivity of this diagnostic method in patients with recent HCoV infections (229E, OC43, and NL63) must be studied further.

In this study, ELISA using N1 or N3 showed high sensitivity and specificity in SARS-CoV antibody testing. These results not only showed that recombinant N protein and its specific monoclonal antibodies may be used as diagnostic reagents for SARS, but also offered a potential target site for the design of an epitope-based vaccine against SARS.

Acknowledgments

This work was supported by grants-in-aid from the Korea food and drug administration and the Korea Research Foundation (KRF-005-E00077). In addition, this work was partially supported through the BK 21 Program for Veterinary Science.

References

1. Che, X. Y., L. W. Qiu, Z. Y. Liao, Y. D. Wang, K. Wen, Y. X. Pan, *et al.* 2005. Antigenic cross-reactivity between severe acute respiratory syndrome-associated coronavirus and human coronaviruses 229E and OC43. *J. Infect. Dis.* **191:** 2033–2037.
2. Dutta, N. K., K. Mazumdar, B. H. Lee, M. W. Baek, D. J. Kim, Y. R. Na, *et al.* 2008. Search for potential target site of nucleocapsid gene for the design of an epitope-based SARS DNA vaccine. *Immunol. Lettl.* **118:** 65–71.
3. Huang, L. R., C. M. Chiu, S. H. Yeh, W. H. Huang, P. R. Hsueh, W. Z. Yang, *et al.* 2004. Evaluation of antibody responses against SARS coronaviral nucleocapsid or spike proteins by immunoblotting or ELISA. *J. Med. Virol.* **73:** 338–346.
4. Marra, M. A., S. J. M. Jones, C. R. Astell, R. A. Holt, A. Brooks-Wilson, Y. S. N. Butterfield, *et al.* 2003. The genome sequence of the SARS-associated coronavirus. *Science* **300:** 1399–1404.
5. Reithinger, R., R. J. Quinnell, B. Alexander, and C. R. Davies. 2002. Rapid detection of *Leishmania infantum* infection in dogs: Comparative study using an immunochromatographic dipstick test, enzyme-linked immunosorbent assay, and PCR. *J. Clin. Virol.* **40:** 2352–2356.
6. Rota, P. A., M. S. Oberste, S. S. Monroe, W. A. Nix, R. Campagnoli, J. P. Icenogle, *et al.* 2003. Characterization of a novel coronavirus associated with severe acute respiratory syndrome. *Science* **300:** 1394–1399.
7. Saijio, M., M. Nikura, S. Morikawa, T. G. Ksiazek, R. F. Meyer, C. J. Peters, and I. Kurane. 2001. Enzyme-linked immunosorbent assay for detection of antibodies to Ebola and Marburg viruses using recombinant nucleoproteins. *J. Clin. Virol.* **39:** 1–7.
8. Saijo, M., T. Ogino, F. Taguchi, S. Fukushi, T. Mizutani, T. Notomi, *et al.* 2005. Recombinant nucleocapsid protein-based IgG enzyme-linked immunosorbent assay for the serological diagnosis of SARS. *J. Virol. Methods* **125:** 181–186.

9. Shang, B., X. Y. Wang, J. W. Yuan, A. Vabret, X. D. Wu, R. F. Yang, *et al.* 2005. Characterization and application of monoclonal antibodies against N protein of SARS-coronavirus. *Biochem. Biophys. Res. Commun.* **336:** 110–117.
10. Shim, Y. Y., W. S. Shin, G. S. Moon, and K. H. Kim. 2007. Quantitative analysis of phosphinothricin-*N*-acetyltransferase in genetically modified herbicide tolerant pepper by an enzyme-linked immunosorbent assay. *J. Microbiol. Biotechnol.* **17:** 681–684.
11. Shin, G. C., Y. S. Chung, I. S. Kim, H. W. Cho, and C. Kang. 2006. Preparation and characterization of a novel monoclonal antibody specific to severe acute respiratory syndrome-coronavirus nucleocapsid protein. *Virus Res.* **122:** 109–118.
12. Sizun, J., D. Soupre, M. C. Legrand, J. D. Giroux, S. Rubio, J. M. Cauvin, C. Chastel, D. Alix, and L. de Parscau. 1995. Neonatal nosocomial respiratory infection with coronavirus: A prospective study in a neonatal intensive care unit. *Acta Paediatr.* **84:** 617–620.
13. Sizun, J., M. W. Yu, and P. J. Talbot. 2000. Survival of human coronaviruses 229E and OC43 in suspension and after drying on surfaces: A possible source of hospital-acquired infections. *J. Hosp. Infect.* **46:** 55–60.
14. Timani, K. A., L. Ye, L. Ye, Y. Zhu, Z. Wu, and Z. Gong. 2004. Cloning, sequencing, expression, and purification of SARS-associated coronavirus nucleocapsid protein for serodiagnosis of SARS. *J. Clin. Virol.* **30:** 309–312.
15. Wang, J., J. Wen, J. Li, J. Yin, Q. Zhu, H. Wang, *et al.* 2003. Assessment of immunoreactive synthetic peptides from the structural proteins of severe acute respiratory syndrome coronavirus. *Clin. Chem.* **49:** 1989–1996.
16. World Health Organization. 2003. WHO post-outbreak biosafety guidelines for handling of SARS-CoV specimens and cultures. Available at http://www.who.int/csr/sars/biosafety2003_12_18/en/.
17. Woo, P. C., S. K. Lau, B. H. Wong, K. H. Chan, W. T. Hui, G. S. Kwan, J. S. Peiris, R. B. Couch, and K. Y. Yuen. 2004. False-positive results in a recombinant severe acute respiratory syndrome-associated coronavirus (SARS-CoV) nucleocapsid enzyme-linked immunosorbent assay due to HCoV-OC43 and HCoV-229E rectified by Western blotting with recombinant SARS-CoV spike polypeptide. *J. Clin. Microbiol.* **42:** 5885–5888.
18. Yu, F., M. Q. Le, S. Inoue, H. T. C. Thai, F. Hasebe, M. del Carmen Parquet, and K. Morita. 2005. Evaluation of inapparent nosocomial severe acute respiratory syndrome coronavirus infection in Vietnam by use of highly specific recombinant truncated nucleocapsid protein-based enzyme-linked immunosorbent assay. *Clin. Diagn. Lab. Immunol.* **12:** 848–854.

Microbiol Immunol 2008; **52**: 625–630
doi:10.1111/j.1348-0421.2008.00079.x

NOTE

Analysis of severe acute respiratory syndrome coronavirus structural proteins in virus-like particle assembly

Mina Nakauchi[1], Hiroaki Kariwa[1], Yasuhiro Kon[2], Kentaro Yoshii[1], Akihiko Maeda[3], and Ikuo Takashima[1]

[1]Laboratory of Public Health, Department of Environmental Veterinary Sciences, [2]Laboratory of Anatomy, Department of Biomedical Sciences and [3]Laboratory of Prion Diseases, Graduate School of Veterinary Medicine, Hokkaido University, Sapporo 060-0818, Japan

ABSTRACT

SARS-CoV has four major structural proteins: the N, S, M, and E proteins. To investigate the mechanism of SARS-CoV assembly, we cloned the genes encoding these four proteins into the eukaryotic expression vector pCAGGS and transfected them into 293T cells. When all four expression vectors were co-transfected VLP formed, as confirmed using electron microscopy. Using a rabbit polyclonal antibody specific to the N protein, N-protein-containing particles similar in size to the VLP were also observed by immunoelectron microscopy, indicating that the VLP contained the N protein. Co-immunoprecipitation analyses demonstrated an interaction between the N and M proteins, suggesting that N protein binds directly to M protein to be incorporated into VLP.

Key words particle formation, SARS-CoV, VLP.

A serious epidemic of SARS, an atypical pneumonia, occurred during 2002 and 2003 (1–3). The novel coronavirus that causes SARS (SARS-CoV) is an enveloped virus with a positive-strand RNA genome of approximately 30 000 nucleotides. The virus particle consists of an RNA genome and four major structural proteins: the N, S, M, and E proteins. Coronaviruses are thought to assemble in the ER–Golgi intermediate compartment through the interaction of structural proteins (4). However, information concerning the interactions of the SARS-CoV structural proteins is extremely limited.

The SARS-CoV N protein is a 46-kDa phosphoprotein that binds to genomic RNA to form a helical ribonucleocomplex that is enveloped by a lipid bilayer containing the S, M, and E proteins (5, 6). It has been proposed that the N protein functions in viral RNA replication and protein translation (7, 8). The S protein is a type-I glycoprotein that plays a role in viral entry by binding to the SARS-CoV receptor, ACE2, which is expressed on the surface of target cells (9). However, the S protein is not thought to be required for virus assembly (10). The M protein, a triple-spanning membrane protein, is the most abundant protein in the virion. The cytoplasmic C-terminal domain of the M protein interacts with the N protein, whereas the N-terminal domain is exposed on the extracellular side of the virion (11, 12). The E protein, which is present in small amounts, is a transmembrane protein that may function as a viroporin (13).

It has recently been reported that low levels of SARS-CoV VLP are released into the culture medium of mammalian cells (10, 14, 15). Because VLP formation resembles virion formation, the mechanism of SARS-CoV particle formation was investigated in the current study by cloning the coding regions for the S, M, E, and N structural

Correspondence
Laboratory of Public Health, Department of Environmental Veterinary Sciences, Graduate School of Veterinary Medicine, Hokkaido University, Kita-18 Nishi-9, Kitaku, Sapporo, Hokkaido 060-0818, Japan.
Tel: +44 11 706 5212; fax: +44 11 706 -5213; email: kariwa@vetmed.hokudai.ac.jp

Received 8 November 2007; revised 18 June 2008; accepted 22 July 2008

List of Abbreviations: ACE2, angiotensin-converting enzyme 2; E, envelope; ELISA, enzyme-linked immunosorbent assay; EM, electron microscopy; ER, endoplasmic reticulum; GFP, green fluorescent protein; HA, hemagglutinin; M, membrane; mAb, monoclonal antibody; MHV, mouse hepatitis virus; N, nucleocapsid; OD, optical density; pAb, polyclonal antibody; PS, packaging signal; RT-PCR, reverse transcriptase polymerase chain reaction; PEG, polyethylene glycol; S, spike; SARS, severe acute respiratory syndrome; SARS-CoV, severe acute respiratory syndrome-associated coronavirus; VLP, virus-like particle.

proteins into the eukaryotic expression vector pCAGGS (16). Primers were designed to add an N-terminal HA tag to the M protein, a C-terminal FLAG tag to the E protein, and a C-terminal HA tag to the S protein. The constructs expressing the M, E, S, and N proteins are designated HA-M-pCAG, E-FLAG-pCAG, S-HA-pCAG, and N-pCAG, respectively.

After co-transfecting 293T cells with HA-M-pCAG, E-FLAG-pCAG, S-HA-pCAG, and N-pCAG, we used EM to confirm the formation of VLP. One hundred nm diameter particles resembling SARS-CoV were visible by EM in the cytoplasm of transfected cells (Fig. 1a). The particles were localized in intracellular vesicles at the periphery of the nucleus (Fig. 1a, arrows) and as buds emerging from the intracellular membrane (Fig. 1b). Similar particles were not detected in normal 293T cells (data not shown).

To confirm the incorporation of N protein into the VLP, we performed an immuno-EM analysis using an N-protein-specific rabbit pAb. Immunofluorescence imaging confirmed that N protein was expressed in the cytoplasm of 293T cells co-transfected with the four expression plasmids (Fig. 1c). By immuno-EM analysis, N-protein-containing particles similar in size to the VLP were visible in intracellular vesicles (Fig. 1d, filled arrowheads), and N protein that was not incorporated into the particles was visible in the cytoplasm (Fig. 1d, open arrowheads). These results confirm that SARS-CoV VLP are produced in cells transfected with the expression plasmids for the M, E, S, and N proteins.

To facilitate the detection of low levels of the structural proteins, we established ELISA. In the N-ELISA, a rabbit anti-N-protein pAb (10 μg/ml) was used for N-protein capture, and an anti-N-protein mAb; (Clone 122) (17) was used at 1:1000 dilution for N-protein detection. In the S-ELISA, an anti-S protein mAb (Clone 341C; Chemicon, Temecula, CA, USA) (18) was used at 1:500 dilution for S-protein capture, and a biotin-conjugated anti-HA-tag mAb (Sigma-Aldrich, St Louis, MO, USA) was used at 1:1000 dilution for S-protein detection.

To determine whether VLP are secreted from 293T cells that express the four structural proteins of SARS-CoV, we analyzed the culture medium of the transfected cells using equilibrium density centrifugation. The N- and S-protein peaks were detected in fraction 6 (Fig. 2) of the 20–50% sucrose gradient. The density of this fraction (1.157 g/cm^3) was similar to that reported previously for VLP-containing fractions (14, 19, 10), indicating that the N and S proteins in fraction 6 were secreted as SARS-CoV VLP. The N protein, but not the S protein, was also detected in fractions 3 and 4 (density, 1.08–1.10 g/cm^3; Fig. 2). The peaks of fractions 3 and 4 may represent aggregates of N protein released from broken cells. These results suggest that SARS-CoV VLP are formed in cells that express

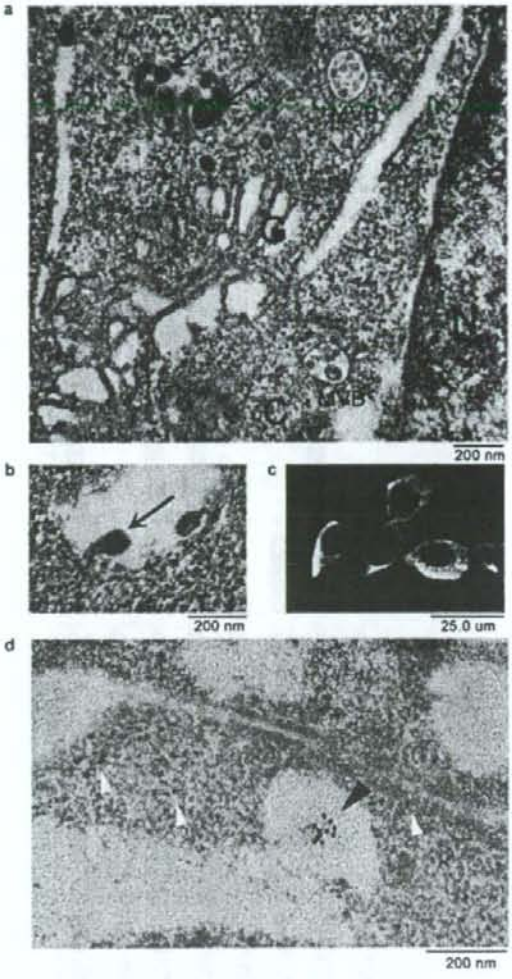

Fig. 1. Analysis of SARS-CoV VLP formation in 293T cells by transmission EM. (a) **Electron micrograph of VLP** (arrows) formed in 293T cells after cells were transfected with expression plasmids for the SARS-CoV M, E, S, and N proteins. Cytoplasm, (C); Golgi, (G); multi-vesicular body, (MVB); nuclei, (N). Scale bar = 200 nm. (b) **Electron micrograph of VLP budding from the intracellular membrane.** Scale bar = 200 nm. (c) **N-protein expression analyzed by indirect immunofluorescence assay.** Cells transfected with the M, E, S, and N expression plasmids were stained with rabbit anti-N-protein pAb. Scale bar = 25.0 μm. (d) **Cells expressing M, E, S, and N proteins analyzed by immuno-EM with rabbit anti-N-protein pAb** (10-nm colloidal gold). Filled and open arrowheads indicate N protein present in particles and cytoplasm, respectively. Scale bar = 200 nm.

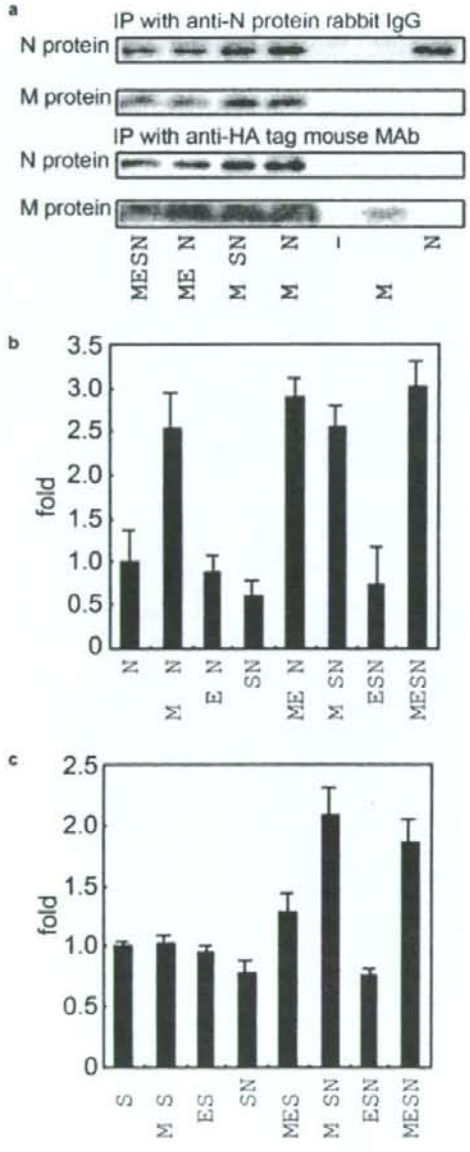

Fig. 2. Equilibrium density analysis of N and S proteins in the culture fluid of 293T cells expressing SARS-CoV structural proteins. Culture fluid collected from cells transfected with HA-M-pCAG, E-FLAG-pCAG, S-HA-pCAG, and N-pCAG was loaded onto a sucrose density gradient, and 1-ml fractions were collected from the bottom of the tubes. Aliquots of the fractions were precipitated with 1.9% NaCl and 10% PEG8000, and the pellets were resuspended in lysis buffer. The 10 fractions collected were analyzed using N- and S-ELISAs. (○) S-ELISA optical density (OD) value; (●) N-ELISA OD value; (■) sucrose concentration (w/w%).

the N, M, E, and S proteins and are secreted into the culture medium. We therefore used the VLP production system and ELISA to analyze the interaction of structural proteins in SARS-CoV particle formation.

In vitro research has shown that the N and M proteins of SARS-CoV interact with each other (11, 20, 21) and that this interaction is important for coronavirus assembly and N-protein incorporation into VLP (22–24). To demonstrate a direct interaction between the N and M proteins, we used immunoprecipitation. When the M and N proteins were co-expressed in 293T cells, they co-precipitated with either anti-N-protein pAb or anti-HA-tag mAb, which recognizes the HA-tagged M protein (Fig. 3a). The S and E proteins did not appear to be required for the N–M protein interaction (Fig. 3a). When either the M or N protein was expressed alone, anti-N-protein pAb did not immunoprecipitate the M protein, and anti-HA-tag mAb did not immunoprecipitate the N protein (Fig. 3a).

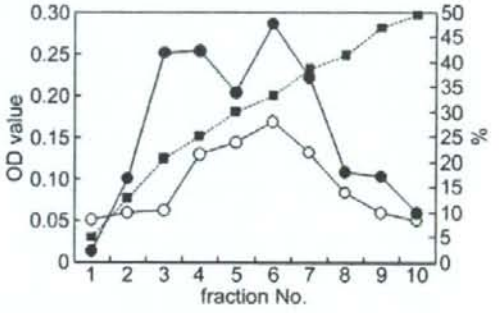

Fig. 3. Interaction between N and M proteins in 293 T cells. Briefly, E-FLAG-pCAG, (E, 3 μg); HA-M-pCAG, (M, 3 μg); N-pCAG, (N, 1 μg); and S-HA-pCAG (S, 2 μg), or a similar amount of empty pCAG vector (–) was transfected into 293T cells using TransIT-LT1 reagent. (a) **Immunoprecipitation analysis.** Transfected cells were lysed using lysis buffer (1% Triton X-100, 0.5% sodium deoxycholate, 0.1% SDS in phosphate-buffered saline), and cell lysates were immunoprecipitated with rabbit anti-N-protein pAb (20 μg/ml; upper two panels) or with anti-HA-tag mAb (lower two panels). The expression plasmids used for transfection are indicated at the bottom of the figure. The viral proteins were analyzed by Western blotting using anti-N-protein mAb (Clone 122) to detect N protein or anti-HA-tag mAb to detect M protein, as indicated to the left of the figure. (b) **N-ELISA results.** The ratio of the extracellular amount of N protein (N-ELISA extracellular OD value) to the total amount of N protein (sum of N-ELISA extra- and intracellular OD values) was calculated for 293T cells that were transfected with the expression plasmids indicated on the x-axis. The results are expressed relative to those from cells that expressed the N protein alone (1). (c) **S-ELISA results.** The ratio of the extracellular amount of S protein to the total amount of S protein was calculated for each sample. The results are expressed relative to those from cells that expressed the S protein alone (1).

The amount of extracellular N protein was significantly increased in cells co-transfected with N-pCAG and HA-M-pCAG (Fig. 3b). The ratio of extracellular N protein to total N protein (the sum of extra- and intracellular N protein) was 2.5 to 3.0 times higher in cells that co-expressed the N and M proteins than in cells that expressed the N protein alone (Fig. 3b). The amount of extracellular S protein was also significantly higher in the cells co-transfected with S-HA-pCAG, HA-M-pCAG, and N-pCAG (Fig. 3c) than in cells transfected with S-HA-pCAG alone. The ratio of extracellular to total S protein (the sum of extra- and intracellular S protein) in the cells that co-expressed the S, M, and N proteins was almost twice that in the cells that expressed the S protein alone (Fig. 3c). The results of the immunoprecipitation analysis suggest that a direct interaction between the M and N proteins is important for the secretion of N and S proteins into the culture medium.

The M and E proteins of MHV have been reported to be essential for virus particle formation and to be sufficient for the production of VLP (25); even the E protein alone has been reported to form VLP (26). Similar studies of SARS-CoV VLP formation have reported conflicting results. Huang *et al.* (10) have reported that the M and N proteins, but not the S and E proteins, are critical for particle formation, whereas Hsieh *et al.* (14) have suggested that the M and E proteins are sufficient for VLP formation. Mortola and Roy (15) have also reported that the M and E proteins, but not the S and N proteins, are required for VLP formation. The latter two reports are consistent with the findings reported for MHV (25).

Our results are in good agreement with those of Huang *et al.* (10), but not with those of Hsieh *et al.* (14) or Mortola and Roy (15). Like Huang *et al.* (10), we used a plasmid-based expression system, whereas Hsieh *et al.* (14) used a vaccinia-T7 polymerase system and Mortola and Roy (15) used a baculovirus system. Therefore, the discrepancies among the reported roles of the SARS-CoV structural proteins in particle formation might be attributable to the use of different experimental expression systems. When viral vectors are used, some other factors might compensate for the function of the N protein.

Coronavirus packaging of genomic RNA is dependent on a nucleotide sequence known as the PS (27, 28). Although packaging of MHV genomic RNA can occur independently of the MHV N protein (29), the MHV N protein does bind to a specific PS sequence located at the end of the *1b* gene of the MHV RNA genome to facilitate its packaging into virus particles (24, 30, 31). Recently, the putative SARS-CoV PS was identified and localized in the genomic region spanning nucleotides 19715–20294, and N-protein expression was demonstrated to be required for packaging of the SARS-CoV genome into VLP (14, 32).

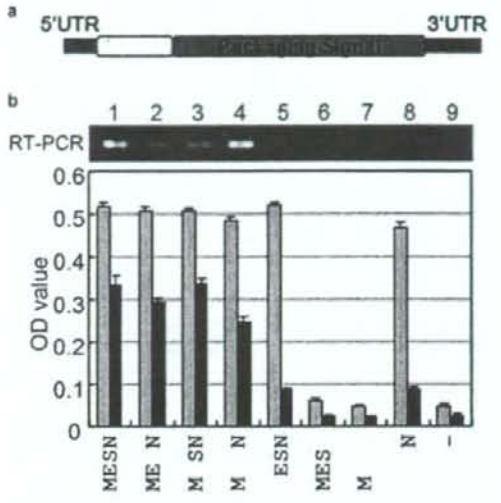

Fig. 4. Analysis of RNA packaging into VLP in 293T cells. (a) **Schematic diagram of synthetic RNA** containing the putative packaging signal of the SARS-CoV (GFP-PS RNA). (b) **Detection of GFP-PS RNA in the culture medium of cells transfected with SARS-CoV structural protein** expression plasmids (as indicated on the x-axis) and then with GFP-PS RNA. After RNase A treatment of the culture medium from transfected cells, the remaining RNA was extracted and subjected to RT-PCR (top of figure). The extracellular (black bars) and intracellular (gray bars) N protein was assayed using N-ELISA.

To validate these earlier reports using our VLP system, we constructed fusion RNA for use in a packaging experiment. This RNA, denoted as GFP-PS RNA (Fig. 4a) contains the SARS-CoV genomic region 18486–21485, which encompasses the putative PS (14). The EGFP gene was transcribed *in vitro* for use as negative-control RNA. Twenty-four hours after transfection with plasmids expressing the SARS-CoV structural proteins, cells were transfected with the *in vitro*-transcribed RNA (2 μg/well) using a TransIT mRNA transfection kit (Mirus, Mississauga, Ontario, Canada) according to the manufacturer's protocol. To elucidate which structural proteins were critical for the release of VLP containing GFP-PS RNA, RT-PCR was carried out using the culture medium from cells that expressed various combinations of the structural proteins (Fig. 4b). Before extraction of total RNA, the PEG-precipitated culture medium was resuspended in PBS supplemented with RNase A (20 μg/ml) and incubated for 30 min at room temperature to degrade free RNA.

GFP-PS RNA was detected in the culture medium of cells co-expressing both the N and M proteins (Fig. 4b, lanes 1–4), but not in that of cells lacking either the M

(lane 5) or the N (lane 6) protein, nor in that of cells expressing only the M (lane 7) or N (lane 8) protein. In contrast, the negative-control EGFP RNA was not detected in the culture medium of cells that co-expressed the M, E, S, and N proteins (data not shown). These results were reproducible in three independent experiments.

The N-ELISA also detected GFP-PS RNA when the N protein was released into the culture medium in the presence of M protein (Fig. 4, lanes 1–4), but not in the absence of M protein (lanes 5 and 8). RNase A-resistant GFP-PS RNA was detected only in the supernatant of cells that expressed both the N and M proteins, conditions that allow the release of the N protein into the culture medium (Fig. 4b). This result suggests that M–N protein interaction is required not only for VLP formation, but also for genome packaging. Given our finding that the M and N proteins interact with each other (Fig. 2a), we surmise that the GFP-PS-bound N protein was packaged into particles by interacting with the M protein and then released into the culture medium.

RNA was detected by RT-PCR, but not by Northern blotting. The putative PS region used in our experiment may be insufficient for efficient packaging of the SARS-CoV genome, or other factors may be required. The SARS-CoV 3a protein, which is thought to be a structural component of the virion, interacts with the 5′-untranslated region of the SARS-CoV genome (33). Therefore, more efficient packaging of the RNA might occur if the 3a protein is also expressed.

We have demonstrated that direct interaction between N and M SARS-CoV proteins is critically important for the formation of VLP and for packaging of the genome into these particles. VLP and ELISA systems should allow more detailed information to be obtained on SARS-CoV particle formation at the molecular level.

ACKNOWLEDGMENTS

We thank Dr Koichi Morita of the Department of Virology, Institute of Tropical Medicine, Nagasaki University, for kindly providing SARS-CoV and Dr Masayuki Okada of Fujirebio (Tokyo, Japan) for supplying the mAb for detection of the SARS-CoV N protein. We also express our gratitude for technical assistance to Miss Mariko Ishizuka of the Laboratory of Public Health, Department of Environmental Veterinary Science, Graduate School of Veterinary Medicine, Hokkaido University. This work was supported by a 21st COE Program of Excellence for Zoonosis Control, a Grant-in-Aid for Scientific Research (no. 18780225 to Nakauchi) from the Ministry of Education, Science, Sports, and Culture of Japan, and the National Project on Protein Structural and Functional Analyses.

REFERENCES

1. Drosten C., Gunther S., Preiser W., van der Werf S., Brodt H.R., Becker S., Rabenau H., Panning M., Kolesnikova L., Fouchier R.A., Berger A., Burguière A.M., Cinatl J., Eickmann M., Escriou N., Grywna K., Kramme S., Manuguerra J.C., Müller S., Rickerts V., Stürmer M., Vieth S., Klenk H.D., Osterhau A.D., Schmitz H., Doerr H.W. (2003) Identification of a novel coronavirus in patients with severe acute respiratory syndrome. *N Engl J Med* **348:** 1967–76.
2. Ksiazek T.G., Erdman D., Goldsmith C.S., Zaki S.R., Peret T., Emery S., Tong S., Urbani C., Comer J.A., Lim W., Rollin P.E., Dowell S.F., Ling A.E., Humphrey C.D., Shieh W.J., Guarner J., Paddock C.D., Rota P., Fields B., DeRisi J., Yang J.Y., Cox N., Hughes J.M., LeDuc J.W., Bellini W.J., Anderson L.J. (2003) A novel coronavirus associated with severe acute respiratory syndrome. *N Engl J Med* **348:** 1953–66.
3. Lee N., Hui D., Wu A., Chan P., Cameron P., Joynt G.M., Ahuja A., Yung M.Y., Leung C.B., To K.F., Lui S.F., Szeto C.C., Chung S., Sung J.J. (2003) A major outbreak of severe acute respiratory syndrome in Hong Kong. *N Engl J Med* **348:** 1986–94.
4. Stertz S., Reichelt M., Spiegel M., Kuri T., Martinez-Sobrido L., Garcia-Sastre A., Weber F., Kochs G. (2007) The intracellular sites of early replication and budding of SARS-coronavirus. *Virology* **361:** 304–15.
5. Marra M.A., Jones S.J., Astell C.R., Holt R.A., Brooks-Wilson A., Butterfield Y.S., Khattra J., Asano J.K., Barber S.A., Chan S.Y., Cloutier A., Coughlin S.M., Freeman D., Girn N., Griffith O.L., Leach S.R., Mayo M., McDonald H., Montgomery S.B., Pandoh P.K., Petrescu A.S., Robertson A.G., Schein J.E., Siddiqui A., Smailus D.E., Stott J.M., Yang G.S., Plummer F., Andonov A., Artsob H., Bastien N., Bernard K., Booth T.F., Bowness D., Czub M., Drebot M., Fernando L., Flick R., Garbutt M., Gray M., Grolla A., Jones S., Feldmann H., Meyers A., Kabani A., Li Y., Normand S., Stroher U., Tipples G.A., Tyler S., Vogrig R., Ward D., Watson B., Brunham R.C., Krajden M., Petric M., Skowronski D.M., Upton C., Roper R.L. (2003) The genome sequence of the SARS-associated coronavirus. *Science* **300:** 1399–404.
6. Rota P.A., Oberste M.S., Monroe S.S., Nix W.A., Campagnoli R., Icenogle J.P., Peñaranda S., Bankamp B., Maher K., Chen M.H., Tong S., Tamin A., Lowe L., Frace M., DeRisi J.L., Chen Q., Wang D., Erdman D.D., Peret T.C., Burns C., Ksiazek T.G., Rollin P.E., Sanchez A., Liffick S., Holloway B., Limor J., McCaustland K., Olsen-Rasmussen M., Fouchier R., Günther S., Osterhaus A.D., Drosten C., Pallansch M.A., Anderson L.J., Bellini W.J. (2003) Characterization of a novel coronavirus associated with severe acute respiratory syndrome. *Science* **300:** 1394–9.
7. Tahara S.M., Dietlin T.A., Nelson G.W., Stohlman S.A., Manno D.J. (1998) Mouse hepatitis virus nucleocapsid protein as a translational effector of viral mRNAs. *Adv Exp Med Biol* **440:** 313–8.
8. Almazan F., Galan C., Enjuanes L. (2004) The nucleoprotein is required for efficient coronavirus genome replication. *J Virol* **78:** 12683–8.
9. Li W., Moore M.J., Vasilieva N., Sui J., Wong S.K., Berne M.A., Somasundaran M., Sullivan J.L., Luzuriaga K., Greenough T.C., Choe H., Farzan M. (2003) Angiotensin-converting enzyme 2 is a functional receptor for the SARS coronavirus. *Nature* **426:** 450–4.
10. Huang Y., Yang Z.Y., Kong W.P., Nabel G.J. (2004) Generation of synthetic severe acute respiratory syndrome coronavirus pseudoparticles: implications for assembly and vaccine production. *J Virol* **78:** 12557–65.
11. He R., Leeson A., Ballantine M., Andonov A., Baker L., Dobie F., Li Y., Bastien N., Feldmann H., Strocher U., Theriault S., Cutts T.,

Cao J., Booth T.F., Plummer F.A., Tyler S., Li X. (2004) Characterization of protein-protein interactions between the nucleocapsid protein and membrane protein of the SARS coronavirus. *Virus Res* **105:** 121–5.
12. Oostra M., de Haan C.A., de Groot R.J., Rottier P.J. (2006) Glycosylation of the severe acute respiratory syndrome coronavirus triple-spanning membrane proteins 3a and M. *J Virol* **80:** 2326–36.
13. Liao Y., Yuan Q., Torres J., Tam J.P., Liu D.X. (2006) Biochemical and functional characterization of the membrane association and membrane permeabilizing activity of the severe acute respiratory syndrome coronavirus envelope protein. *Virology* **349:** 264–75.
14. Hsieh P.K., Chang S.C., Huang C.C., Lee T.T., Hsiao C.W., Kou Y.H., Chen I.Y., Chang C.K., Huang T.H., Chang M.F. (2005) Assembly of severe acute respiratory syndrome coronavirus RNA packaging signal into virus-like particles is nucleocapsid dependent. *J Virol* **79:** 13848–55.
15. Mortola E., Roy P. (2004) Efficient assembly and release of SARS coronavirus-like particles by a heterologous expression system. *FEBS Lett* **576:** 174–8.
16. Niwa H., Yamamura K., Miyazaki J. (1991) Efficient selection for high-expression transfectants with a novel eukaryotic vector. *Gene* **108:** 193–9.
17. Kogaki H., Uchida Y., Fujii N., Kurano Y., Miyake K., Kido Y., Kariwa H., Takashima I., Tamashiro H., Ling A.E., Okada M. (2005) Novel rapid immunochromatographic test based on an enzyme immunoassay for detecting nucleocapsid antigen in SARS-associated coronavirus. *J Clin Lab Anal* **19:** 150–9.
18. Tripp R.A., Haynes L.M., Moore D., Anderson B., Tamin A., Harcourt B.H., Jones L.P., Yilla M., Babcock G.J., Greenough T., Ambrosino D.M., Alvarez R., Callaway J., Cavitt S., Kamrud K., Alterson H., Smith J., Harcourt J.L., Miao C., Razdan R., Comer J.A., Rollin P.E., Ksiazek T.G., Sanchez A., Rota P.A., Bellini W.J., Anderson L.J. (2005) Monoclonal antibodies to SARS-associated coronavirus (SARS-CoV): identification of neutralizing and antibodies reactive to S, N, M and E viral proteins. *J Virol Methods* **128:** 21–8.
19. Huang C., Ito N., Tseng C.T., Makino S. (2006) Severe acute respiratory syndrome coronavirus 7a accessory protein is a viral structural protein. *J Virol* **80:** 7287–94.
20. Fang X., Ye L., Timani K.A., Li S., Zen Y., Zhao M., Zheng H., Wu Z. (2005) Peptide domain involved in the interaction between membrane protein and nucleocapsid protein of SARS-associated coronavirus. *J Biochem Mol Biol* **38:** 381–5.
21. Luo H., Wu D., Shen C., Chen K., Shen X., Jiang H. (2006) Severe acute respiratory syndrome coronavirus membrane protein interacts with nucleocapsid protein mostly through their carboxyl termini by electrostatic attraction. *Int J Biochem Cell Biol* **38:** 589–99.
22. Hurst K.R., Kuo L., Koetzner C.A., Ye R., Hsue B., Masters P.S. (2005) A major determinant for membrane protein interaction localizes to the carboxy-terminal domain of the mouse coronavirus nucleocapsid protein. *J Virol* **79:** 13285–97.
23. Kuo L., Masters P.S. (2002) Genetic evidence for a structural interaction between the carboxy termini of the membrane and nucleocapsid proteins of mouse hepatitis virus. *J Virol* **76:** 4987–99.
24. Narayanan K., Maeda A., Maeda J., Makino S. (2000) Characterization of the coronavirus M protein and nucleocapsid interaction in infected cells. *J Virol* **74:** 8127–34.
25. Vennema H., Godeke G.J., Rossen J.W., Voorhout W.F., Horzinek M.C., Opstelten D.J., Rottier P.J. (1996) Nucleocapsid-independent assembly of coronavirus-like particles by co-expression of viral envelope protein genes. *EMBO J* **15:** 2020–8.
26. Maeda J., Maeda A., Makino S. (1999) Release of coronavirus E protein in membrane vesicles from virus-infected cells and E protein-expressing cells. *Virology* **263:** 265–72.
27. Makino S., Yokomori K., Lai M.M. (1990) Analysis of efficiently packaged defective interfering RNAs of murine coronavirus: localization of a possible RNA-packaging signal. *J Virol* **64:** 6045–53.
28. Fosmire J.A., Hwang K., Makino S. (1992) Identification and characterization of a coronavirus packaging signal. *J Virol* **66:** 3522–30.
29. Narayanan K., Chen C.J., Maeda J., Makino S. (2003) Nucleocapsid-independent specific viral RNA packaging via viral envelope protein and viral RNA signal. *J Virol* **77:** 2922–7.
30. Narayanan K., Makino S. (2001) Cooperation of an RNA packaging signal and a viral envelope protein in coronavirus RNA packaging. *J Virol* **75:** 9059–67.
31. Woo K., Joo M., Narayanan K., Kim K.H., Makino S. (1997) Murine coronavirus packaging signal confers packaging to nonviral RNA. *J Virol* **71:** 824–7.
32. Qin L., Xiong B., Luo C., Guo Z.M., Hao P., Su J., Nan P., Feng Y., Shi Y.X., Yu X.J., Luo X.M., Chen K.X., Shen X., Shen J.H., Zou J.P., Zhao G.P., Shi T.L., He W.Z., Zhong Y., Jiang H.L., Li Y.X. (2003) Identification of probable genomic packaging signal sequence from SARS-CoV genome by bioinformatics analysis. *Acta Pharmacol Sin* **24:** 489–96.
33. Sharma K., Surjit M., Satija N., Liu B., Chow V.T., Lal S.K. (2007) The 3a accessory protein of SARS coronavirus specifically interacts with the 5′UTR of its genomic RNA, using a unique 75 amino acid interaction domain. *Biochemistry* **46:** 6488–99.

Japanese Journal of Veterinary Research 56(3): 151-165, 2008

FULL PAPER

Genetic and antigenic analyses of a Puumala virus isolate as a potential vaccine strain

Nur Hardy Abu Daud[1)], Hiroaki Kariwa[1),*)], Evgeniy Tkachenko[2)], Tamara Dzagurnova[2)], Olga Medvedkina[2)], Petr Tkachenko[2)], Mariko Ishizuka[1)], Takahiro Seto[1)], Daisuke Miyashita[1)], Takahiro Sanada[1)], Mina Nakauchi[1)], Kentaro Yoshii[1)], Akihiko Maeda[3)], Kumiko Yoshimatsu[4)], Jiro Arikawa[4)], and Ikuo Takashima[1)]

[1)]Laboratory of Public Health, Graduate School of Veterinary Medicine, Hokkaido University, Sapporo 060-0818, Japan

[2)]Russian Academy of Medical Sciences, Chumakov Institute of Poliomyelitis and Viral Encephalitides, Moscow 142782, Russia.

[3)]Department of Prion Diseases, Graduate School of Veterinary Medicine, Hokkaido University, Sapporo 060-0818, Japan

[4)]Department of Microbiology, Graduate School of Medicine, Hokkaido University, Sapporo 060-8638, Japan

Received for publication, October 23, 2008; accepted, November 18, 2008

Abstract

Puumala virus (PUUV), a causative agent of hemorrhagic fever with renal syndrome (HFRS), is prevalent in Europe and European Russia. No vaccine has been developed for PUUV-associated HFRS, primarily because of the low viral yield in cultured cells. A PUUV strain known as DTK/Ufa-97 was isolated in Russia and adapted for growth in Vero E6 cells maintained in serum-free medium. The DTK/Ufa-97 strain produced a higher viral titer in serum-free medium, suggesting that it may prove useful in the development of an HFRS vaccine. When PUUV-infected Vero E6 cells were grown in serum-free medium, the DTK/Ufa-97 strain yielded more copies of intracellular viral RNA and a higher viral titer in the culture fluid than did the Sotkamo strain. Phylogenetic analysis revealed that PUUVs can be classified into multiple lineages according to geographical origin, and that the DTK/Ufa-97 strain is a member of the Bashkiria-Saratov lineage. The deduced amino acid sequences of the small, medium, and large segments of the DTK/Ufa-97 strain were 99.2% to 100%, 99.3% to 99.8%, and 99.8% identical, respectively, to those of the Bashkirian PUUV strains and 96.9%, 92.6%, and 97.4% identical, respectively, to those of the Sotkamo strain, indicating that the PUUVs are genetically diverse. However, DTK/Ufa-97 and other strains of PUUV exhibited similar patterns of binding to a panel of monoclonal antibodies against Hantaan virus. In addition, diluted antisera (i.e., ranging from 1:160 to 1:640) specific to three strains of PUUV neutralized both homologous and heterologous viruses. These results suggest that the DTK/Ufa-97 strain is capable of extensive growth and is antigenically similar to genetically distant strains of PUUV.

Key words: hantavirus, hemorrhagic fever with renal syndrome, Puumala virus, vaccine

*Corresponding auther: Hiroaki Kariwa, Laboratory of Public Health, Department of Environmental Veterinary Sciences, Graduate School of Veterinary Medicine, Hokkaido University, Sapporo 060-0818, Japan.
Phone: +81-11-706-5212. Fax: +81-11-706-5213. E-mail: kariwa@vetmed.hokudai.ac.jp

Introduction

Hantaviruses belong to the genus *Hantavirus*, within the family *Bunyaviridae*. These viruses cause two zoonoses: hemorrhagic fever with renal syndrome (HFRS) and hantavirus pulmonary syndrome (HPS). Hemorrhagic fever with renal syndrome is caused by Hantaan virus (HTNV), Seoul virus (SEOV), Puumala virus (PUUV), Dobrava-Belgrade virus (DOBV), and Amur virus (AMRV), and occurs primarily in Asia and Europe. HPS occurs in the Americas and is caused by Sin Nombre virus (SNV), Andes virus (ANDV) and other hantaviruses[14,24,26]. Hantaviruses are transmitted via aerosolized excretions of rodents in the family *Muridae*. Their viral genomes contain large (L), medium (M), and small (S) segments of negative-stranded RNA, which encode a viral RNA-dependent RNA polymerase, a glycoprotein precursor, and a nucleocapsid protein (NP), respectively[27].

Five viruses are known to cause human HFRS in Russia. Specifically, PUUV and DOBV cause HFRS in European Russia[31], while HTNV, SEOV, and AMRV cause HFRS in Far Eastern Russia[18,21,29,36]. Sporadic cases of PUUV-and DOBV-induced HFRS were recently detected in the western Siberian regions of Russia[35]. The principal hosts for HTNV, AMRV, SEOV, and PUUV are *Apodemus agrarius*, *Apodemus peninsulae*, *Rattus norvegicus*, and *Myodes glareolus*, respectively. Detailed phylogenetic analyses of strains from Europe have shown that DOBV strains derived from *Apodemus flavicollis* form a separate evolutionary lineage (i.e., DOBV-Af), while strains derived from *A. agrarius* are more diverse. Strains from central Europe and central European Russia form the DOBV-Aa lineage, and are distinct from the Saaremaa strains of northeastern Europe[10,11]. In the Sochi district of southern Russia, a previously unknown DOBV variant (i.e., DOBV-Ap) was identified in *Apodemus ponticus*, a novel hantavirus host, and determined to cause HFRS[12,32]. Although the DOBV strains from *Apodemus* hosts in European Russia and Europe share high amino acid sequence similarity, phylogenetic analyses in humans and an animal model reveal that they form separate lineages with distinct virulence traits[13]. A novel DOBV-Ap lineage associated with *A. ponticus* emerged in an area south of European Russia, confirming the reputation of DOBV as the most virulent of the European hantaviruses[12].

Approximately 200,000 cases of HFRS are reported worldwide each year[4], including 150,000 cases in China[3,16], 600 to 1,000 cases in Korea[8], 1,000 cases in Finland, and 200 cases in Sweden[22,33]. In Russia, HFRS has the highest incidence and morbidity of all human zoonotic virus infections. Approximately 6,000 to 8,000 clinical cases of HFRS are reported in European Russia every year. Of these, most are caused by PUUV and a smaller fraction are caused by DOBV. As the strains of HFRS in European Russia are caused by several distinct hantaviruses and vary in severity, it is inappropriate to refer to the disease as 'nephropathia epidemica'. Consequently, the WHO Working Group proposed the term 'hemorrhagic fever with renal syndrome' to describe similar clinical syndromes in Russia, Europe and Asia[34].

HFRS can be prevented by reducing exposure to live rodents and their excreta. However, rodent control measures are expensive and difficult to maintain over long periods, as it would be impossible to completely eradicate the viral hosts. Hence, immunization would be the most effective way to decrease HFRS morbidity in endemic regions of Russia.

Several commercial hantavirus vaccines are produced in China and Korea[4,37]. These vaccines are effective against HTNV and SEOV infections, but do not provide immunity to antigenically distinct PUUVs. No vaccine has been developed against PUUV, primarily because of the low viral yield in cultured cells. A potential vaccine strain (i.e., DTK/Ufa-97) was isolated from a patient with HFRS during a large 1997 outbreak in the Bashkiria region of Russia[23]. High titers of the virus were prepared in Vero E6 cells grown in serum-free medium (SFM). Here, we perform genetic and antigenic characterizations of the DTK/Ufa-97 strain.

Materials and Methods

Cell lines and culture media: Vero E6 cells were purchased from American Type Culture Collection (Manassas, VA, USA) and cultivated in Eagle's minimum essential medium (MEM; Invitrogen, Carlsbad, CA, USA) supplemented with 2 mM L-glutamine (Sigma, St. Louis, MO, USA), 10% fetal bovine serum (FBS), 100 IU/ml penicillin, and 100 μg/ml streptomycin (penicillin-streptomycin) (Cambrex, East Rutherford, NJ, USA). Vero E6 cells were adapted to SFM via growth in virus production (VP)-SFM (Invitrogen) containing 2 mM L-glutamine for 2 months.

Viral strains: The potential vaccine strain (i.e., DTK/Ufa-97) was isolated in 1997 from a deceased HFRS patient in Bashkiria, Russia and was adapted to Vero E6 cells grown in SFM. Two other PUUV strains were used, including a prototype Sotkamo strain that originated from *M. glareolus* in Finland[28] and a Kazan strain that originated from *M. glareolus* in Kazan, Russia[6,19]. Strains 76-118[15], SR-11[9], and H5[18] were used as representative HTNV, SEOV, and AMRV strains, respectively. All virus strains were propagated in Vero E6 cells prior to use.

Plaque assay: Freshly trypsinized Vero E6 cells (i.e., 1×10^6 cells/well) were seeded into the flat-bottom wells of six-well Multiwell Cell Culture Plates (BD Biosciences, San Jose, CA, USA). The medium was aspirated from the cultures and 0.2 ml aliquots of serial 10-fold viral dilutions were inoculated into the wells. The viruses were allowed to adsorb for 1 hr at 37℃, whereupon 10 ml of an overlay mixture [i.e., Eagle's MEM "Nissui 1" (Nissui Pharmaceutical Co., Ltd., Ueno, Tokyo, Japan) supplemented with 2 mM L-glutamine (Sigma), 10% FBS, and 1.5% SeaKem GTG Agarose (Cambrex)] was added to each well. After one week, 2 ml of a 0.025% solution of Neutral Red (Wako, Osaka, Japan) in overlay medium was added to each well. The wells were examined for plaques 7 days after staining.

Sampling for analysis of PUUV replication: Vero E6 cells grown in MEM and Vero E6 cells adapted to SFM were used to assess PUUV replication. The cells were infected with DTK/Ufa-97 or Sotkamo and cultured for 21 days. Culture fluids and infected cells were collected at 2, 6, 12, and 21 hours post-infection and at 3, 7, 10, 14, 17, and 21 days post-infection (dpi). The culture medium was changed every 7 days. The collected fluids were centrifuged at 1,200 rpm for 5 min, and the supernatants were stored at -80℃ as viral stocks. Infected cells were collected in MEM or SFM using a cell scraper. The cells were then suspended and centrifuged at 1,200 rpm for 5 min. The resulting cell pellets were stored at -80℃ until further use.

Indirect immunofluorescence assay: Monoclonal antibodies (MAbs) specific to glycoproteins Gn and Gc of strain HTNV 76-118[11] were obtained from mouse ascitic fluid and used in indirect immunofluorescence assay (IFA) for the antigenic characterization of DTK/Ufa-97. Hantavirus-infected Vero E6 cells were spotted onto 24 well slides. The slides were incubated for 4 hr at 37℃, fixed in cold acetone for 20 min, washed in phosphate-buffered saline (PBS) and distilled water, air dried, and stored at -40℃ until further use. Diluted MAbs (i.e., 1:10 to 1:1,000,000) derived from the hybridoma or ascitic fluids were spotted onto the slides, which were then incubated for 1 hr at 37℃ and washed three times with PBS. The slides were then incubated in Alexa Fluor 488-conjugated goat anti-mouse IgG (i.e., final dilution =1:1,000; Invitrogen) for 1 hr at 37℃. The slides were washed and 90% glycerol was applied. The IFA titer of each MAb was expressed as the reciprocal of the maximum antibody dilution that yielded granular and scattered fluorescence in the cytoplasm.

Focus assay and titration of viruses: Approximately 2×10^5 Vero E6 cells/ml MEM (i.e., 0.5 ml/well) were seeded into eight chamber slides (Iwaki, Nihonbashi, Tokyo, Japan), maintained in a CO_2 incubator overnight, and infected with serially di-

luted stocks of Sotkamo or DTK/Ufa-97 strains. After adsorption for 1 hr in a CO_2 incubator, the virus inoculum was removed and MEM containing 1.5% carboxymethyl cellulose sodium salts (Wako) was layered onto the cells at a concentration of 0.6 ml/well. The cells were then cultured in a CO_2 incubator for 14 days at 37℃.

The resulting viral foci were visualized by IFA. Briefly, the cultured Vero E6 cells were washed three times with PBS, fixed with 0.2 ml/well of methanol for 20 min under UV light in a safety cabinet in a BSL3 laboratory. After removing methanol, the slides were thoroughly air-dried, and washed with PBS. The slides were then incubated in anti-PUUV hamster serum (i.e., final dilution=1:1,000) for 1 hr at 37℃, washed, and incubated with Alexa Fluor 488-conjugated goat anti-hamster IgG (i.e., final dilution=1:1,000; Invitrogen) for 1 hr. After washing, 90% glycerol was applied to the slides, and the viral foci were counted and measured under a fluorescence microscope. The focus diameters were expressed in μm, and the viral titers were expressed as focus-forming units/ml (i.e., ffu/ml).

Focus reduction neutralization test: The endpoint titers of the neutralizing antibodies were determined using focus reduction neutralization test (FRNT). Hamster immune sera specific to PUUV strains DTK/Ufa-97, Kazan, and Sotkamo; and mouse immune sera specific to HTNV strain 76-118, AMRV strain H5, and SEOV strain SR-11 were used to compare the antigenicity of DTK/Ufa-97 to that of other PUUV and hantavirus strains. Serial 2-fold dilutions of immune sera (30 μl) were mixed with equal volumes of viral stock (i.e., 60 ffu /30 μl) and incubated for 1 hr at 37℃. The mixture was then used to inoculate Vero E6 cell monolayers grown in 96-well flat-bottom plates at a concentration of 50 μl/well (Nunc TM, Roskilde, Denmark). After adsorption for 1 hr at 37℃, the inocula were removed and MEM containing 1.5% carboxymethyl cellulose sodium salts was layered onto the cells (i.e., 200 μl/well). The cells were cultured in a CO_2 incubator for 7 days at 37℃, washed with PBS, fixed with methanol, and air-dried.

The fixed cells were incubated with MAb E5/G6 (i.e., final dilution=1:200)[38] for 1 hr at 37℃. After three washes with PBS, the cells were incubated with Alexa Fluor 488-conjugated goat anti-mouse IgG (i.e., final dilution=1:1,000) for 1 hr at 37℃. The stained foci were counted under a fluorescence microscope, and the FRNT titer was defined as the highest dilution of serum associated with at least an 80% reduction in focus formation.

RNA isolation and reverse transcription: Total RNA was isolated from DTK/Ufa-97-infected Vero E6 cells using Isogen (Nippon Gene), according to the manufacturer's protocol. In preparation for first-strand cDNA synthesis, 11 μl of the extracted RNA (i.e., 5 μg) was mixed with 1 μl of random primers (i.e., 3 μg/μl, Invitrogen) and 1 μl of 10 mM dNTPs (TaKaRa, Otsu, Japan). The mixture was heated at 70℃ for 10 min, cooled to 25℃ over the span of 10 min, and chilled on ice for 3 min. Reverse transcription was performed via the addition of 4 μl of 5× first-strand buffer (Invitrogen), 2 μl of 0.1 mM DTT, and 1 μl of SuperScript II (200 U/μl, Invitrogen). The cDNA synthesis reaction was allowed to proceed for 50 min at 42℃, and was stopped by heating at 70℃ for 15 min.

Real-time polymerase chain reaction: Before cDNA synthesis for real-time polymerase chain reaction (PCR), RNA was treated with DNase. Briefly, 15 μg RNA was mixed with 5 μl of 10× DNase buffer (TaKaRa), 2 μl of RNase-free DNase I (5 U/μl; TaKaRa), 0.5 μl of RNase Out ribonuclease inhibitor (40 U/μl; Invitrogen), and double-distilled water (DDW) to a final volume of 50 μl. The tubes were incubated for 30 minutes at 37℃, precipitated with lithium chloride (Ambion, Austin, TX, USA), and dissolved in 30 μl of DDW. The DNase-treated RNA was used for cDNA synthesis as described above.

Real-time PCR was then performed on the DNase-treated samples. Primers and minor groove binder (MGB) probes specific to the PUUV

S segment were designed using Primer Express software (ver. 2.0; Applied Biosystems, Foster City, CA, U.S.A.), and probes were labeled with 5' reporter dye, 6-Carboxyfluorescein (FAM) and a 3'-MGB/non-fluorescent quencher. After optimization of the primer and probe concentrations, samples were assayed in quadruplicate 25 μl reactions. Each reaction contained 2.25 μl of cDNA, 12.5 μl of 2× TaqMan Universal PCR Master Mix (Applied Biosystems), 0.225 μl each of 100 μM forward and reverse primers (i.e., Sotkamo62Fw: 5' -TCCAAGA GGATATAACCCGCCAT-3' and Sotkamo257Rv: 5'-TTCCTGGACACAGCATCTGC-3', respectively), 0.46 μl of 10.9 μM fluorescent probe (i.e., Sotkamo 194: 5'-TGTCAGCACTGGAGGA-3'), and 9.34 μl of DDW. Samples were incubated at 50℃ for 2 min and 95℃ for 10 min, followed by 60 thermal cycles of 95℃ for 15 sec and 60℃ for 1 min. Real-time data were collected using the 7000 Sequence Detection System (Applied Biosystems).

Real-time PCR data were normalized to rodent GAPDH expression. The same amount of cDNA (i.e. 2.25 μl) was mixed with 12.5 μl of 2× TaqMan Universal PCR Master Mix, 0.25 μl each of 10 μM rodent GAPDH forward and reverse primers, and 0.25 μl of 20 μM rodent GAPDH probe (VIC-labeled). All primers and probes were purchased from Applied Biosystems.

Nucleotide sequencing analysis: The cDNA derived from the total RNA of DTK/Ufa-97-infected Vero E6 cells was amplified using Platinum® Taq DNA polymerase high fidelity (Invitrogen), according to the manufacturer's instructions. The reaction mixture also contained 2 pmol of primers specific to the S, M, and L segments of the DTK/Ufa-97 strain, in a final volume of 25 μl. After an initial denaturation step (i.e., 94℃ for 2 min), the cDNA was amplified via 35 thermal cycles of 94℃ for 30 sec, 55℃ for 30 sec, and 68℃ for 4 min.

The 3'- and 5'-ends of the S, M, and L segments were amplified using RNA isolated from the infected-cell culture medium and the 5' RACE System for Rapid Amplification of cDNA Ends (ver. 2.0; Invitrogen). In preparation for 5'-end amplification, randomly primed synthetic cDNA was dCTP-tailed using a terminal deoxynucleotidyl transferase. The tailed cDNA was amplified using a 5' RACE abridged anchor primer (AAP, Invitrogen) and PUUV-specific primers. In preparation for 3'-end amplification, the isolated RNA was CTP -tailed using poly(A) polymerase (Ambion), and the tailed RNA was reverse-transcribed using AAP and SuperScript™ II (Invitrogen). The cDNA was amplified using PUUV-specific primers and an abridged universal amplification primer (Invitrogen).

The amplified products were electrophoresed in agarose gels, stained with ethidium bromide, and visualized under UV light. The DNA fragments were excised from the gel and purified using the Wizard SV Gel and PCR Clean-up System (Promega, Madison, WI, USA), according to the manufacturer's instructions. Purified DNA fragments were directly sequenced at least two times in the forward and reverse directions using the ABI-PRISM Dye Terminator Sequencing Kit and the ABI 3130 Genetic Analyzer (both from Applied Biosystems).

Phylogenetic analysis: Hantavirus nucleotide (nt) and deduced amino acid sequences were compared using Genetyx software (ver. 8). The ClustalX program package (ver. 2.0) was used to generate a phylogenetic tree using the neighbor-joining method with 1,000 bootstrap replicates.

Statistical analysis: The viral RNA copies in infected Vero E6 cells and virus titers in cultured media were compared by Student's t-test. P values of 0.05 or less were considered statistically significant.

Results

Plaque and focus formation by PUUV strain DTK/Ufa-97

To examine the plaque-and focus-forming abilities of DTK/Ufa-97, Vero E6 monolayers were inoculated with virus and the resulting plaques

and foci were enumerated. Vero E6 cells infected with DTK/Ufa-97 exhibited small plaques (average diameter=1 mm to 2 mm) at 14 days post-infection, whereas cells infected with the PUUV Sotkamo strain did not form plaques (data not shown). In addition, the DTK/Ufa-97 foci (average diameter ± S.D., 196 μm±46 μm) were more than twice as large as the Sotkamo foci (average diameter ± S.D., 80 μm±6 μm) (data not shown).

Viral RNA copy number and virus titer

The DTK/Ufa-97-infected Vero E6 cells and the corresponding culture media were collected at various intervals after infection, and the viral RNA copy number and viral titer were determined. Viral RNA expression remained unchanged in Vero E6 cells grown in MEM, with approximately 1×10^3 to 7×10^3 copies of viral RNA transcribed during the 24 hr following infection. The copy number increased to approximately 5×10^4 copies at 3 dpi and remained at that level until 21 dpi (Fig. 1). In comparison, Sotkamo RNA replication occurred more slowly, reaching a plateau level at 7 dpi. When SFM was used instead of MEM, the DTK/Ufa-97 RNA copy number increased to 2.4×10^5 by 14 dpi and remained at that level until 21 dpi. However, fewer than 4×10^3 copies of Sotkamo RNA were present at 21 dpi.

When Vero E6 cells were grown in MEM, the DTK/Ufa-97 viral titer reached a peak of 2.8×10^5 ffu/ml at 7 dpi, then decreased to 1.4×10^4 ffu/ml at 10 dpi and remained unchanged until 21 dpi (Fig. 2). In contrast, the Sotkamo titer reached a peak of 2.1×10^4 ffu/ml at 7 dpi, then declined to 6.0×10^3 ffu/ml at 10 dpi and remained unchanged until 21 dpi. When Vero E6 cells were grown in SFM, the DTK/Ufa-97 titer reached peaks of 4.5×10^4, 8.3×10^4, and 9.3×10^4 ffu/ml at 7, 14, and 21 dpi,

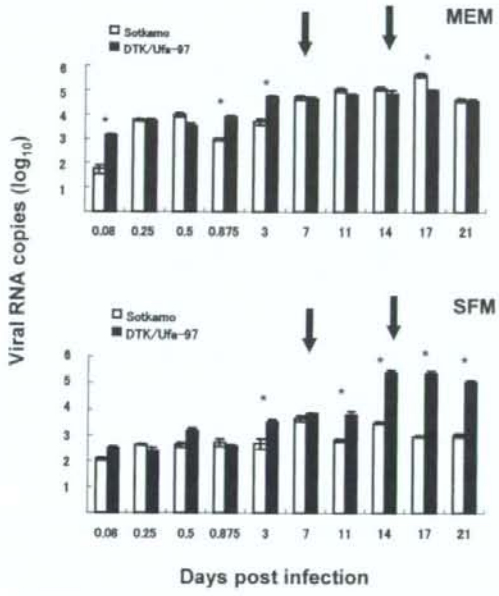

Fig. 1. Copy numbers of PUUV RNA in infected Vero E6 cells.
Cells were infected with PUUV strains Sotkamo and Ufa-97 at a multiplicity of infection (MOI) of 0.02, and were then maintained in MEM containing 10% FBS (*MEM*) or in *SFM*. Viral RNA copy numbers were determined via quadruplicate real-time PCR experiments. The number of viral RNA copies in infected cells is expressed as log10 of the RNA copy number. The standard deviation for each virus is shown at the top of the column corresponding to RNA copy number. Arrows indicate times when the medium was changed. Asterisks indicate significant differences, as determined using Student's t-tests (defined by $P < 0.05$).

respectively, whereas the Sotkamo titer remained less than 3.1×10^3 ffu/ml throughout the observation period.

Sequencing of the complete DTK/Ufa-97 genome

The full-length S, M, and L segments of the DTK/Ufa-97 genome were sequenced, and the resulting data were deposited into the DNA Data Bank of Japan under accession numbers AB 297665, AB297666, and AB297667, respectively. To our knowledge, this is the first complete genomic sequence of a human PUUV isolate from Russia. The S, M, and L segments of the DTK/Ufa-97 strain were 1,829, 3,682, and 6,550 nts in length, respectively (data not shown). These sequences differ from those of the Sotkamo genome only in the length of the S segment, which was 1 nt longer in Sotkamo strain (data not shown).

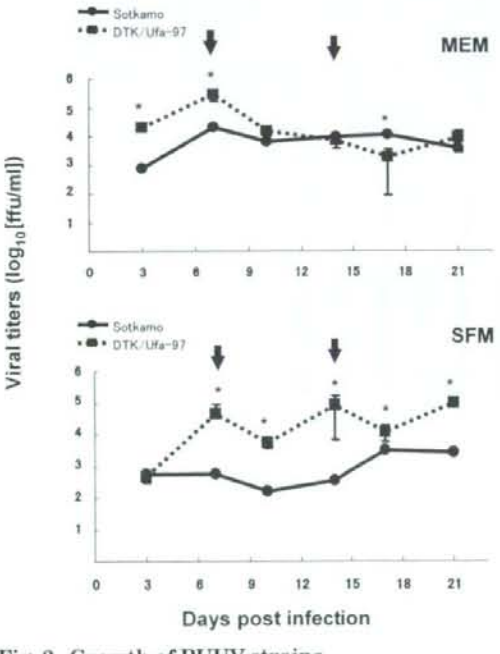

Fig. 2. Growth of PUUV strains.
Vero E6 cells were infected with Sotkamo or DTK/Ufa-97 at an MOI of 0.02 and maintained in either MEM or SFM. Supernatants were collected at the indicated times. The viral titer in the supernatant fraction was expressed as log_{10} [ffu/ml], and titers for each virus were determined in IFA triplicates. The standard deviation for each virus is shown at the top of the viral titer column. Arrows indicate the time points at which the medium was changed. Asterisks indicate significant differences, as determined using Student's t-tests (defined by $P < 0.05$).

Amino acid and nucleotide sequence comparisons

The nucleotide sequence of the DTK/Ufa-97 S segment was 99.9%, 100%, 99.5%, 99.5%, 93.9%, 93.9%, and 85.3% identical to the sequences of PUUV strains CG1820, P360, K27, CG17, Fs808, Kazan, and Sotkamo, respectively. Nucleotide sequence identity was greater than 93% among the Russian PUUVs; however, the Russian and Finnish PUUV Sotkamo strains were approximately 84% identical (Table 1). The predicted amino acid sequences of all of the PUUVs, including the Sotkamo strain, were more than 96% identical (Table 1).

The nucleotide sequence of the DTK/Ufa-97 M segment was 99.6%, 99.8%, 99.8%, 99.4%, 85.8%, 82.8%, and 80.3% identical to those of PUUV strains CG1820, P360, K27, CG17, Kazan, Sotkamo, and Umea/hu, respectively (Table 2). The M segments of the Bashkirian viruses, including DTK/Ufa-97, were more than 99% identical at the nucleotide level, whereas the M segments of the Bashkirian and Northern European strains were approximately 80.3% to 83.2% identical. The Russian PUUV M segments were more than 94.5% identical at the amino acid level, whereas the entire group of PUUV M segments were more than 88% identical (Table 2).

The PUUV L segments were more than 81% identical at the nucleotide level, while the amino acid sequences of the L segment were at least 93% identical among all PUUVs (Table 3).

Phylogenetic analyses

We examined the evolutionary relationship between DTK/Ufa-97 and other hantaviruses by performing phylogenetic analyses of the S, M, and L genome segments using the neighbor-joining method. The DTK/Ufa-97 strain was determined to be a member of the PUUV group, and all three

segments of the DTK/Ufa-97 strain were determined to be members of the Russia/Bashkiria-Saratov lineage (Figs. 3A and 3B). The PUUV branching patterns were consistent with geographical origin, and PUUVs from European Russia (i.e., including the Bashkiria-Saratov, Tataria, and Samara PUUVs from the Volga river region) occupied a single cluster. The Russian/Omsk PUUVs clustered with the Sotkamo strain (Fig. 3A).

Table 1. Nucleotide and amino acid identities of the hantavirus S segment[a].

		ucleotide identities (%)									
		Puumala virus (PUUV)								HTNV[b]	SNV[c]
		Ufa-97[d,e]	CG1820	P360[e]	K27[e]	CG17	Fs808[e]	Kazan	Sot[f]	76-118	NM-H10
VUUP	Ufa-97	–	99.9	100	99.5	99.5	93.9	93.9	85.3	62.2	67.8
	CG1820	99.7	–	99.9	99.4	94.4	93.8	93.8	85.2	62.1	67.8
	P360	100	99.7	–	99.5	99.5	93.9	93.9	85.2	62.2	67.7
	K27	99.2	98.9	99.2	–	99.1	93.5	93.5	85.0	62.0	67.3
	CG17	100	99.7	100	99.2	–	94.2	94.4	85.5	62.7	67.5
	Fs808	99.4	99.2	99.4	98.6	99.4	–	94.8	84.6	62.6	67.8
	Kazan	98.9	98.6	98.9	98.0	98.9	98.9	–	84.5	62.5	68.1
	Sotkamo	96.9	96.6	96.9	96.3	96.9	96.9	96.8	–	63.3	66.7
	HTNV	59.3	59.0	59.3	58.4	59.3	59.6	59.3	59.6	–	61.3
	SNV	69.7	69.9	69.7	69.1	69.7	69.9	69.9	69.1	61.4	–
		Amino acid identities (%)									

[a] Nucleotide region to be compared : nt 172-1,239
[b] Hantaan virus
[c] Sin Nombre virus
[d] DTK/Ufa-97 strain
[e] PUUV originated from HFRS patients
[f] Sotkamo strain

Table 2. Nucleotide and amino acid identities of the hantavirus M segment[a].

		Nucleotide identities (%)									
		Puumala virus (PUUV)								HTNV[b]	SNV[c]
		Ufa-97[d,e]	CG1820	P360[e]	K27[e]	CG17	Kazan	Sot[f]	Umea[e]	76-118	NM-H10
VUUP	Ufa-97	–	99.6	99.8	99.8	99.4	85.8	82.8	80.3	60.0	66.7
	CG1820	99.3	–	99.5	99.5	99.1	85.7	82.8	80.3	60.1	66.7
	P360	99.8	92.3	–	99.9	99.3	86.0	83.1	80.5	60.2	66.9
	K27	99.7	99.1	99.7	–	99.4	86.3	83.2	80.8	60.5	67.3
	CG17	99.6	99.0	99.6	99.6	–	86.0	83.1	80.5	60.1	66.6
	Kazan	95.0	94.5	95.1	96.8	95.2	–	84.7	80.6	59.5	66.0
	Sotkamo	92.6	92.2	92.7	94.2	92.7	93.2	–	80.7	59.0	66.7
	Umea	88.9	88.4	88.9	91.1	89.1	89.4	89.3	–	59.8	65.9
	HTNV	53.4	51.9	52.2	54.0	53.3	54.5	53.6	51.8	–	58.9
	SNV	65.5	64.5	64.8	67.2	64.8	64.0	64.7	64.0	54	–
		Amino acid identities (%)									

[a] Nucleotide region to be compared: nt 53-3,494
[b] Hantaan virus
[c] Sin Nombre virus
[d] DTK/Ufa-97 strain
[e] PUUV originated from HFRS patients
[f] Sotkamo strain

Table 3. Nucleotide and amino acid identities of the hantavirus L segment[a].

		Nucleotide identities (%)							
		Puumala virus (PUUV)					HTNV[b]	SEOV[c]	SNV[d]
		Ufa-97[e,f]	CG1820	Kazan	Sot[g]	Umea[f]	76-118	80-39	NM-H10
VUUP	Ufa-97	—	99.8	87.1	84.5	81.3	67.0	67.1	71.0
	CG1820	99.8	—	87.1	84.6	81.4	67.0	67.2	71.0
	Kazan	99.1	98.9	—	85.0	81.9	67.1	66.9	71.7
	Sotkamo	97.4	97.2	97.4	—	82.1	66.8	67.8	71.3
	Umea	93.9	93.8	94.1	93.2	—	66.5	66.3	69.9
	HTNV	68.8	68.8	68.8	68.6	67.2	—	74.3	66.7
	SEOV	68.5	68.3	68.2	68.4	66.8	84.7	—	67.1
	SNV	77.8	77.1	77.4	77.6	76.1	68.9	68.9	—
		Amino acid identities (%)							

[a] Nucleotide region to be compared: nt 52-6,524
[b] Hantaan virus
[c] Seoul virus
[d] Sin Nombre virus
[e] DTK/Ufa-97 strain
[f] PUUV originated from HFRS patients
[g] Sotkamo strain

Table 4. Antigenic characteristic of Ufa-97 and other hantavirus strains.

MAbs against glycoprotein of HTNV	Antigenic site	IFA titer[a]					
		Puumala			Hantaan	Amur	Seoul
		Ufa-97[b]	Kazan	Sotkamo	76-118	H5	SR-11
8B6	Gn-a (1)	—	—	—	+++	+++	+
6D4	Gn-a (2)	—	—	—	—	—	—
10F11	Gn-a (2)	+	+	—	++	+++	+
2D5	Gn-b	—	—	—	++	++	+
3D5	Gn-b	—	—	—	+	+	+
16D2	Gn-b	—	—	—	++	++	—
HCO2	Gc-a (1)	—	—	—	++	++++	++++
16E6	Gc-a (2)	—	—	—	++	+++	++
EB06	Gc-b	+	+	+	++	+++	+
11E10	Gc-c	+++	+++	++	+++	+++	—
17G6	Gc-d	+	+	+	++	+++	+
5B7	Gc-d	++	+++	++	+++	+++	+++
20D3	Gc−e	+	+	—	++	+++	—
8E10	Gc-f(1)	+++	+++	+++	++	+++	++
1G8	Gc-f(1)	+++	+++	++	+++	+++	++
3B6	Gc-f(1)	+++	+++	+	+++	++	++
23G10-1	Gc-f(2)	—	—	—	++	++	++
7G6	Gc-f(2)	—	—	—	++	+++	++
18F5	Gc-f(2)	—	—	—	++	+++	+

[a] Antibody reactivity is defined as: −,<1:10; +,1:10; ++,1:100; +++,1:1,000; ++++,>1:1,000
[b] DTK/Ufa-97 strain

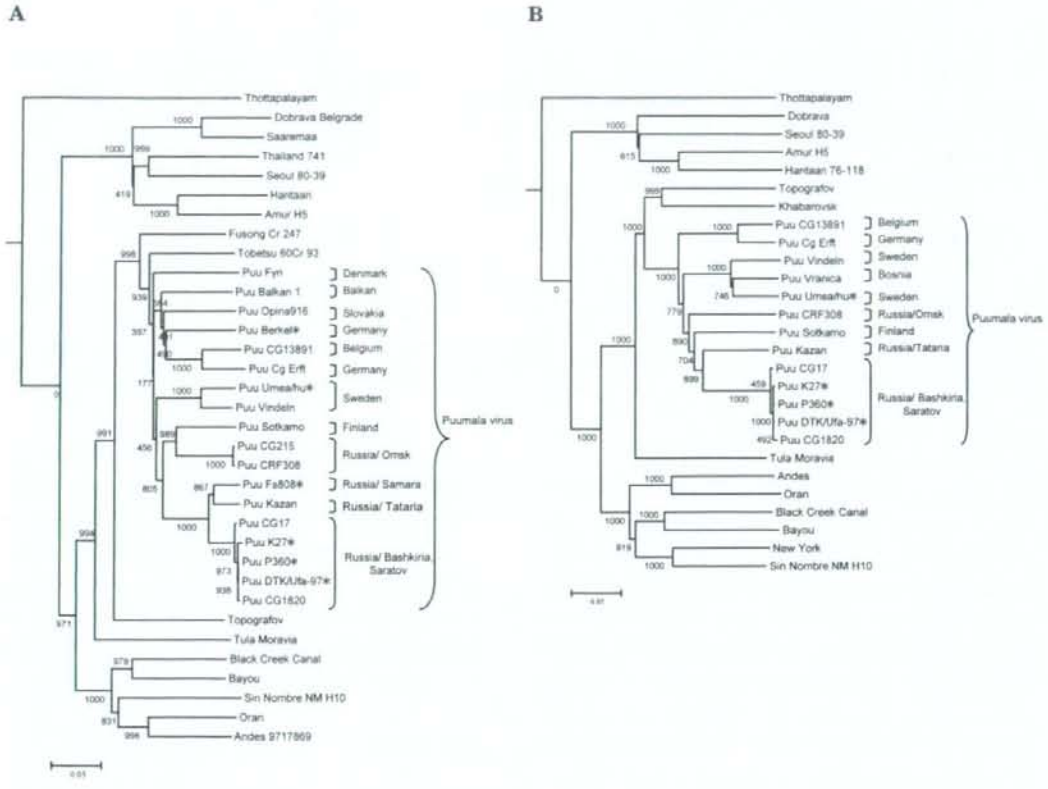

Fig. 3. Phylogenetic analysis of hantaviruses.
The nt sequences of the S, M, and L segments were obtained from the Genome Sequence Database. Multiple sequence alignment was performed using ClustalX software (ver. 2.0), and a phylogenetic tree was derived using the neighbor-joining method. Bootstrap values resulting from 1,000 replications are listed above each branch. A) Phylogenetic analysis of the 1068 nt S segment (i.e., approximately nucleotides 172 to 1239). The accession numbers for the S segment sequences are as follows: Thottapalayam, AY526097; Dobrava Belgrade, L41916; Saaremaa, AJ616854; Thailand 741, AB186420; Seoul 80-39, AY273791; Hantaan, M14626; Amur H5,AB127996; Fusong Cr 247, EF442087; Tobetsu 60Cr 93, AB010731; Puu Fyn, AJ238791; Puu Balkan1,AJ314600; Puu Opina 916, AF294652; Puu Berkel, L36943; Puu CG13891, U22423; Puu Cg-Erft, AJ238779; Puu Umea/hu, AY526219; Puu Vindeln/L20Cg/83, Z48586; Puu Sotkamo, X61035; Puu CG215, AF367066; Puu CRF308, AF367070; Puu F-s 808, AF411446; Puu Kazan, Z84204; Puu CG17/Baskiria-2001, AF442613; Puu K27, L08804; Puu P360, L11347; Puu DTK/Ufa-97, AB297665; Puu CG1820, M32750; Topografov, AJ011646; Tula Moravia/5302v/95, Z69991; Black Creek Canal, L39949; Bayou, L36929; Sin Nombre NM H10, L25784; Oran 22996, AF482715; and Andes Chile-9717869, AF291702. B) Phylogenetic tree of the 3442 nt viral M segment (i.e., approximately nucleotides 53 to 3494). The M segment accession numbers are as follows: Thottapalayam VRC-66412, EU001329; Dobrava-Belgrade DOBV/Ano-Poroia/Af19/1999, AJ410616; Seoul 80-39, S47716; Amur H5,AB127993; Hantaan 76-118, Y 00386; Topografov, AJ011647; Khabarovsk, AJ011648; Puu CG13891, U22418; Puu Cg-Erft, AJ238778; Puu Vindeln, Z49214; Puu Vranica, U14136; Puu Umea/hu, AY526218; Puu CRF308/Omsk, AF442617; Puu Sotkamo, X 61034; Puu Kazan, Z84205; Puu CG17/Baskiria-2001, AF442614; Puu K27, L08754; Puu P360, L08755; Puu DTK /Ufa97, AB297666; Puu CG1820, M29979; Tula Moravia/5302v/95, Z69993; Andes Chile-9717869, AF291703; Oran O122996, AF028024; Black Creek Canal, L39950; Bayou, L36930; New York NY-2,U36803; and Sin Nombre NM H10, L25783. Asterisks indicate viral strains of human origin.

Table 5. Cross-focus reduction neutralization titers of immune sera specific Ufa-97 and other representative hantaviruses.

Serum	Virus					
	Puumala			Hantaan	Amur	Seoul
	Ufa-97[a]	Kazan	Sotkamo	76-118	H5	SR-11
Ufa-97	160[b]	160	160	40	40	20
Kazan	160	160	320	80	80	20
Sotkamo	160	160	640	80	20	20
Hantaan	40	20	20	160	20	40
Amur	40	40	20	80	160	20
Seoul	20	<10	20	20	20	40

[a] DTK/Ufa-97 strain
[b] Neutralizing antibody titers to the homologous viruses are shaded and bold. Titers are shown as the reciprocal of the dilution that resulted in at least 80% reduction in focus, compared with the control (i.e., no antibody)

Antigenic characteristics of DTK / Ufa-97

The antigenic profile of the DTK/Ufa-97 strain was compared with that of other hantaviruses using IFA with a MAb panel. Six of the MAbs used in this study were specific to the HTNV envelope Gn glycoprotein, while 13 were specific to the Gc glycoprotein (Table 4). All MAbs specific to HTNV glycoproteins cross-reacted with AMRV, yielding very similar patterns. In addition, some MAbs specific to HTNV glycoproteins cross-reacted with SEOV, yielding somewhat dissimilar patterns (Table 4). Of the MAbs specific to antigenic sites of the Gn-a, Gn-b, Gn-a, and Gn-f(2) envelope glycoproteins, only MAb 10F11 cross-reacted with any of the PUUV strains. However, MAbs specific to the antigenic sites of the Gc-b, Gc-c, Gc-d, Gc-e, and Gc-f(1) glycoproteins reacted with all hantaviruses tested, including the PUUV strains (Table 4). In general, the PUUV strains exhibited similar reaction patterns to the latter group of MAbs (Table 4).

Cross-neutralization test

To further investigate the antigenic characteristics of DTK/Ufa-97, hamsters were infected with the DTK/Ufa-97, Kazan, and Sotkamo strains and immune sera were collected. These sera were then used to neutralize homologous or heterologous PUUV strains. All sera proved effective at high neutralizing titers (i.e., dilutions of 1:160 to 1:640) (Table 5). The PUUV immune sera exhibited lower neutralizing titers against HTNV, AMRV, and SEOV. However, immune sera specific to HTNV, AMRV, and SEOV exhibited high neutralizing antibody titers to homologous viruses but lower titers to heterologous viruses. These results indicate that the antigenic properties of DTK/Ufa-97 are similar to those of other PUUVs, with regards to the induction of neutralizing antibodies.

Discussion

Hemorrhagic fever with renal syndrome has the highest incidence and morbidity of all human zoonotic viral infections in Russia. Approximately 97% of HFRS cases are caused by PUUV in the European regions of Russia, whereas 3% of HFRS cases are caused by HTNV, SEOV and AMRV in the far-Eastern regions of the country[18,30]. An HFRS vaccine is urgently needed, as morbidity rates are high and approximately 12.5 million people (i.e., 25% of the population) in European regions are at risk for PUUV infection. Several hantavirus vaccines have been produced; however, none are effective against PUUV-induced HFRS. The difficulties in developing a PUUV vaccine stem from the low viral yield in cell culture. High titers of a potential vaccine strain, known as DTK/Ufa-97, can be cultured in SFM-grown Vero E6 cells. Here, we demonstrate that the DTK/Ufa-97 strain yields more viral RNA in infected Vero E6

cells and higher viral titers in the culture fluid of infected cells, when compared with the Sotkamo strain (Figs. 1 and 2). Our data clearly indicate that the DTK/Ufa-97 strain replicates more efficiently than the Sotkamo strain in SFM-cultured Vero E6 cells, as well as in MEM supplemented with FBS.

Minimum essential medium supplemented with FBS has been empirically shown to provide good conditions for cell growth and is commonly used in the formulation of growth media. However, FBS is a potential carrier of infectious agents such as fungi, bacteria, viruses, and prions, which could contaminate a final vaccine preparation[2]. Therefore, SFM is a safer alternative, as it does not contain components of animal or human origin. Several cell lines, including BHK-21[7] and Vero cells[17], have been successfully established in SFM.

A lot of PUUV sequences have been deposited in the DNA database, however, few full-length PUUV genome sequences are available, particularly for human isolates. Therefore, we determined the full-length nucleotide sequence of the DTK/Ufa-97 strain. To our knowledge, this is the first characterization of a Russian PUUV isolate from an HFRS patient. Our phylogenetic analysis revealed that the DTK/Ufa-97 strain is closely related to PUUV strains from the same geographic region (i.e., Bashkiria-Saratov) (Fig. 3). Our analysis identified four Russian PUUV clusters: Bashkiria-Saratov, Tataria, Samara, and Omsk (Fig. 3A). The first three clusters appeared on the same branch, while the Omsk cluster was more closely related to the Finland virus than to the other Russian viruses. This result is consistent with a previous report, in which the genetic identities of Russian and Finnish PUUV strains strongly correlated with their geographic origins[5,25].

The identities of predicted amino acid sequences in the S, M, and L segments were approximately 96.3%, 92.2%, and 93.2%, respectively among all PUUVs. However, the nucleotide sequences identities of the S, M, and L segments were much lower (i.e., approximately 84.5%, 80.3%, and 81.3%, respectively) (Tables 1-3). Few studies have examined the antigenic properties of PUUV; thus, we also examined the antigenic characteristics of DTK/Ufa-97 using MAbs. We compared the antigenicity of three PUUV strains (i.e., DTK/Ufa-97, Kazan, and Sotkamo), as well as other hantaviruses. The reaction patterns exhibited by the DTK/Ufa-97 strain were strikingly similar to those of other Russian and Finnish PUUVs (Table 4), but different than those of other hantaviruses, especially with regards to the Gn protein.

Envelope glycoproteins are presumed to play a major role in the induction of protective immunity and neutralizing antibodies[1,20]. Our cross-neutralization test demonstrated that a neutralizing antibody specific to the DTK/Ufa-97 strain also neutralized other PUUV strains at almost same antibody titer. In addition, antibodies to other PUUV strains cross-neutralized the DTK/Ufa-97 strain and homologous viruses (Table 5). Although the various PUUVs exhibit geographic-dependent genetic variation, they seem to share similar antigenic properties. Therefore, the DTK/Ufa-97 strain may prove useful in inducing protective immunity against a variety of PUUV strains, and may aid in the development of a DTK/Ufa-97-based vaccine.

Our findings revealed that the PUUV strain DTK/Ufa-97 grows well in Vero E6 cells cultured in SFM, and that it is antigenically similar to other PUUVs. These data may aid in the development of a PUUV vaccine strain based on DTK/Ufa-97.

Acknowledgments

We thank Dr. Junko Maeda for her useful suggestions and excellent technical support. We also appreciate the technical advice provided by Dr. Richard Yanagihara (University of Hawaii) and Satoru Arai (National Institute of Infectious Diseases, Japan) regarding our efforts to sequence the 3'- and 5'- ends of the hantavirus genome. This study was supported in part by Grants-in-Aid for Scientific Research (16405034 and 17255009) from the Japanese Ministry of Education, Culture,